Supplementary Information

One-step synthesis of epitaxial 3D/2D metal halide perovskite heterostructures

Zhaohua Zhu, Shaoyu Zeng, Qian Chen, Lei Yang, Cong Wei, Bo Chen, Haidong Yu, Hai Li, Jian Zhang, Xiao Huang**

Experimental section

Materials: CsBr (cesium bromide, 99.999%), $PbBr_2$ (lead (II) bromide, 99.999%) and 1-octadecene (ODE, 90%) were purchased from Sigma-Aldrich (Germany). PEABr (phenethylammonium bromide, ≥ 99.5%), PEAI (phenethylammonium iodide, ≥ 99.5%), PEACl (phenethylammonium chloride, ≥ 99.5%), BABr (butylammonium bromide, ≥99.5%) and PMABr (phenmethylammonium bromide, ≥99.5%) were purchased from Xi' an Polymer Light Technology Co., Ltd. (China). Cs_2CO_3 (cesium carbonate, 99.9%), OA (oleic acid, 85%) and OLA (oleylamine, 90%) were purchased from Aladdin (China). Toluene (analytical reagent) and N,N-dimethylformamide (DMF, analytical reagent) were purchased from Shanghai Chemical Reagent Co., Ltd. (China). All chemicals were used as purchased.

One-step synthesis of epitaxial $CsPbBr_3/PEA_2PbBr_4$ heterostructures: In a typical process of synthesis of $CsPbBr_3/PEA_2PbBr_4$ heterostructures, the precursor solution was prepared by dissolving PEABr (0.07 mmol), CsBr (0.015 mmol) and $PbBr_2$ (0.05 mmol) in DMF solution (1 mL) with stirring. Then the as prepared precursor solution (100 μL) was quickly injected into a toluene solution (5 mL) under vigorous stirring. The $CsPbBr_3/PEA_2PbBr_4$ heterostructures were obtained after centrifugation at 8000 rpm and thoroughly washed with toluene for 3 times. The product was dispersed in toluene for future use. Other kinds of heterostructures were synthesized by replacing PEABr with PEACl, PEAI, PMABr or BABr with other procedure unchanged. The concentration of $CsPbBr_3$ and PEA_2PbBr_4 in the $CsPbBr_3/PEA_2PbBr_4$ heterostructures solution were determined by the atomic absorption spectroscopy (AAS) measurement.

Synthesis of PEA_2PbBr_4 nanoplates: Typically, a precursor solution was prepared by dissolving PEABr (0.1 mmol) and $PbBr_2$ (0.05 mmol) in DMF (1 mL). Then the as prepared precursor solution (100 μL) was quickly added into a toluene solution (5 mL) under vigorous stirring. The PEA_2PbBr_4 nanoplates were obtained after centrifugation at 8000 rpm and thoroughly washed with toluene for 3 times. The obtained perovskite nanoplates were dispersed in toluene for future use. Other kinds of nanoplates were synthesized by replacing PEABr with PEACl, PEAI, PMABr or BABr. The concentration of PEA_2PbBr_4 solution was determined by the AAS measurement.

Synthesis of OA/OLA capped $CsPbBr_3$ nanocubes: First, Cs_2CO_3 (0.407 g) and OA (1.25 mL) were mixed with ODE (15 mL) in a 100 mL three-neck flask. The mixture was heated to 120 ^oC under vacuum for 60 min to remove water and oxygen. Afterwards, the temperature was increased to 150 ^oC in an Ar environment until all Cs_2CO_3 was totally reacted with OLA and

form an optically clear solution. After 30 min, the solution was cooled down to room temperature and stored as stock solution. The temperature was kept at 120 °C before injection. Then, ODE (5 mL), $PbBr_2$ (0.069 g), OA (0.5 mL) and OLA (0.5 mL) were mixed in a 50 mL three-neck bottle. Water and oxygen were removed under vacuum for 20 min. The temperature was increased to 160 °C in an Ar environment and kept for 20 min until $PbBr_2$ had completely dissolved. Afterward, 0.4 mL of the Cs-oleate precursor was quickly injected. After 5 seconds, the three-neck bottle was placed in an ice bath and cooled to room temperature. The final products were washed with toluene and centrifuged off by 8000 rpm for 3 times. The obtained perovskite nanocubes were dispersed in toluene for future use. The concentration of $CsPbBr_3$ solution were determined by the AAS measurement.

Synthesis of physically mixed $CsPbBr_3/PEA_2PbBr_4$ heterostructures: Based on the AAS measurement, similar ratio of $CsPbBr_3$ and PEA_2PbBr_4 solution were physically mixed compared to the epitaxial heterostructure, and stirred at 1000 rpm for 10 min. The obtained products were washed with toluene and centrifuged off at 8000 rpm for 3 times and redispersed in certain volume of toluene to obtain similar concentration as in the epitaxial heterostructures.

Fabrication of photodetectors and photo-response measurements: Au interdigitated electrodes (10 μm electrode interval) on Si/SiO_x substrates were purchased from Guangzhou Mecart Sensor Technology Co., Ltd. (China). The concentration of perovskite solutions for fabricating photodetectors were determined by AAS. Then, the photodetectors were fabricated by dropping solutions of the as prepared $CsPbBr_3/PEA_2PbBr_4$ heterostructures, PEA_2PbBr_4 nanoplates, $CsPbBr_3$ nanocubes and the physically mixed $CsPbBr_3/PEA_2PbBr_4$ heterostructures on the electrodes. A Keithley 4200 Semiconductor Parametric Analyzer (Keithley, USA) was used to measure the photoresponse of the photodetectors in air at room temperature. 405 nm and 450 nm lasers were used for the measurements. A LP1 power meter (Sanwa Electric Instrument Co., Ltd., Japan) was used to measure the power intensity of the laser.

Characterizations: Transmission electron microscope (TEM, JEOL 2100 Plus, Japan) operated at 200 kV and high-resolution transmission electron microscope (HRTEM, JEOL 2100F, Japan) operated at 200 kV were used to characterize the morphology of the products. The structure of products was studied by X-ray diffraction (XRD, SmartLab Rigaku, Japan, with Cu Kα radiation at $\lambda = 1.54$ Å). A UV-vis spectrophotometer (UV-1750, Shimadzu, Japan), F4600 fluorescence spectrometer (Hitachi, Japan) and FLSP920 fluorescence spectrophotometer (Edinburgh Instruments, England) were used to characterize the optical properties of products. In-situ PL measurement was recorded with a USB2000 spectrometer (Ocean Optics, USA) during dropping one droplet of the perovskite precursor solution into a toluene solution. A 365 nm UV light was used as the excitation source. STEM imaging, EDX mapping and line scan were implemented with a Cs-corrected TEM (JEM-ARM300F Grand ARM, Japan) operated at 300 kV.

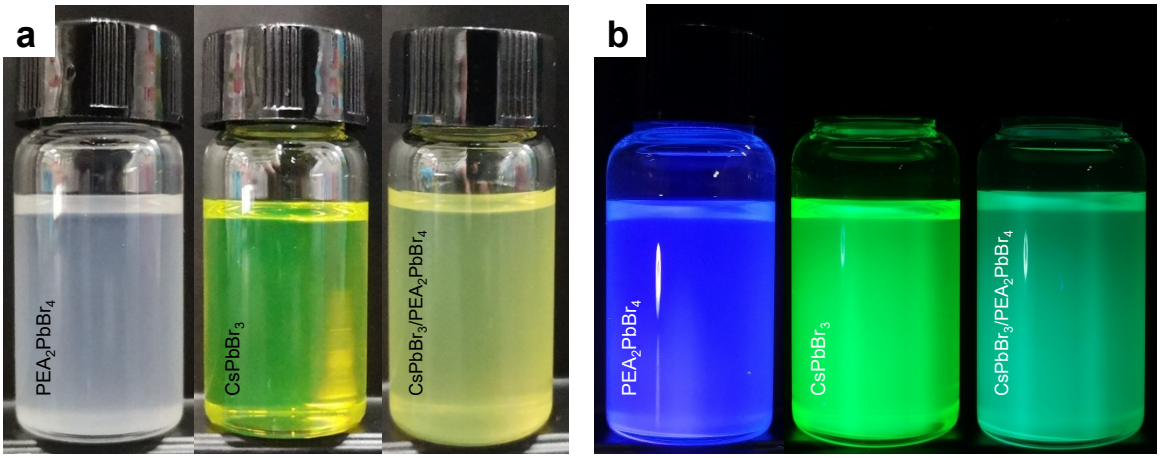

Fig. S1 Photographs of PEA_2PbBr_4 nanoplates, $CsPbBr_3$ nanocubes and $CsPbBr_3/PEA_2PbBr_4$ heterostructures under (a) day light and (b) UV light.

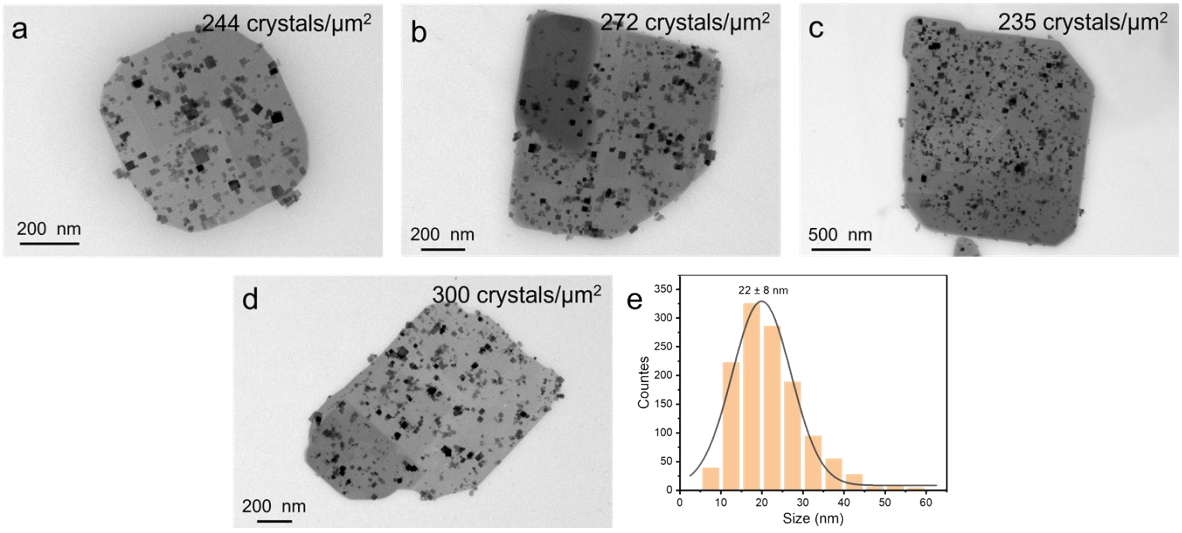

Fig. S2 (a-d) TEM images of typical $CsPbBr_3/PEA_2PbBr_4$ heterostructures and (e) size distribution analysis.

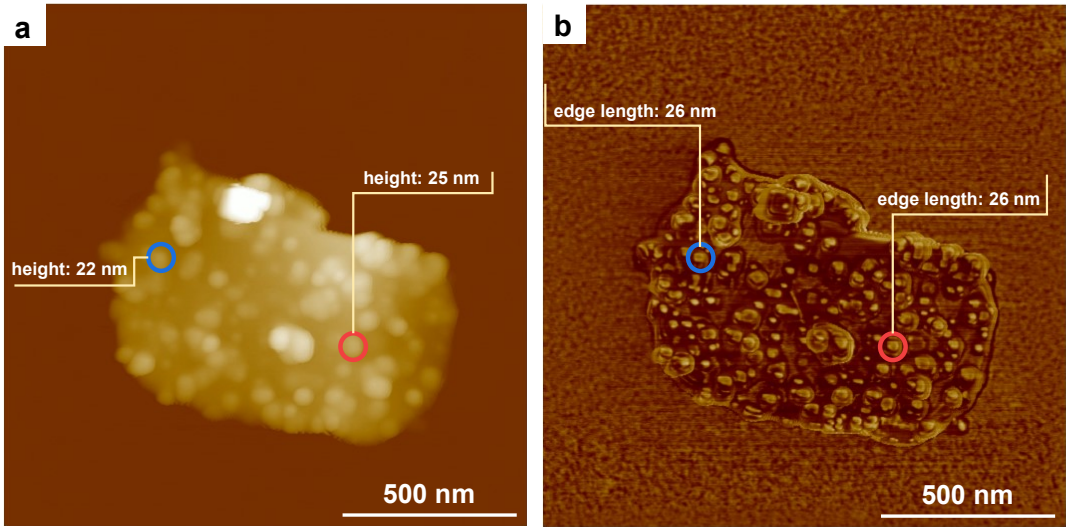

Fig. S3 AFM (a) height and (b) phase image of a typical $CsPbBr_3/PEA_2PbBr_4$ heterostructures.

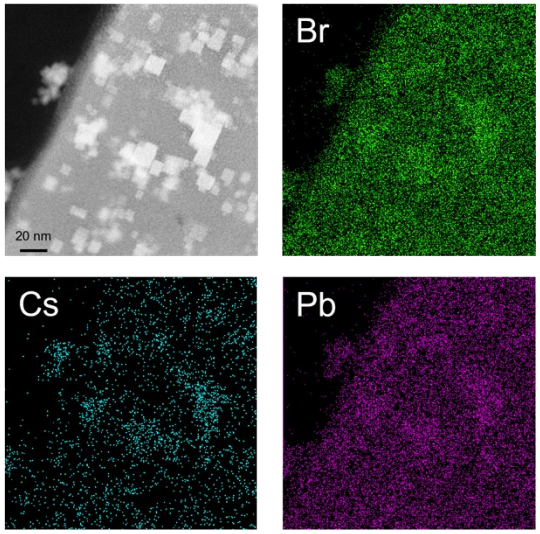

Fig. S4 STEM image and EDX mapping of a $CsPbBr_3/PEA_2PbBr_4$ heterostructures.

As shown in Fig. S5a below, the epitaxial heterostructure shows a seamless contact line between PEA_2PbBr_4 and $CsPbBr_3$. For comparison, in the random heterostructure (Fig. S5b), PEA_2PbBr_4 and $CsPbBr_3$ perovskites were separated by an uneven organic layer with a gap ranging from 1.5 to 3.0 nm. These results indicate that the heterointerface can be controlled by using different preparation methods.

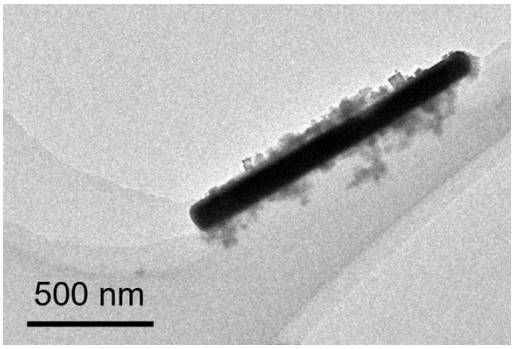

Fig. S5 TEM images of vertical standing $CsPbBr_3/PEA_2PbBr_4$ heterostructures.

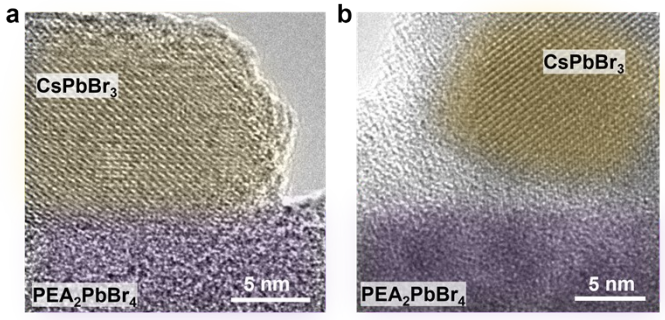

Fig. S6 HRTEM images of (a) epitaxial and (b) random $CsPbBr_3/PEA_2PbBr_4$ heterostructure.

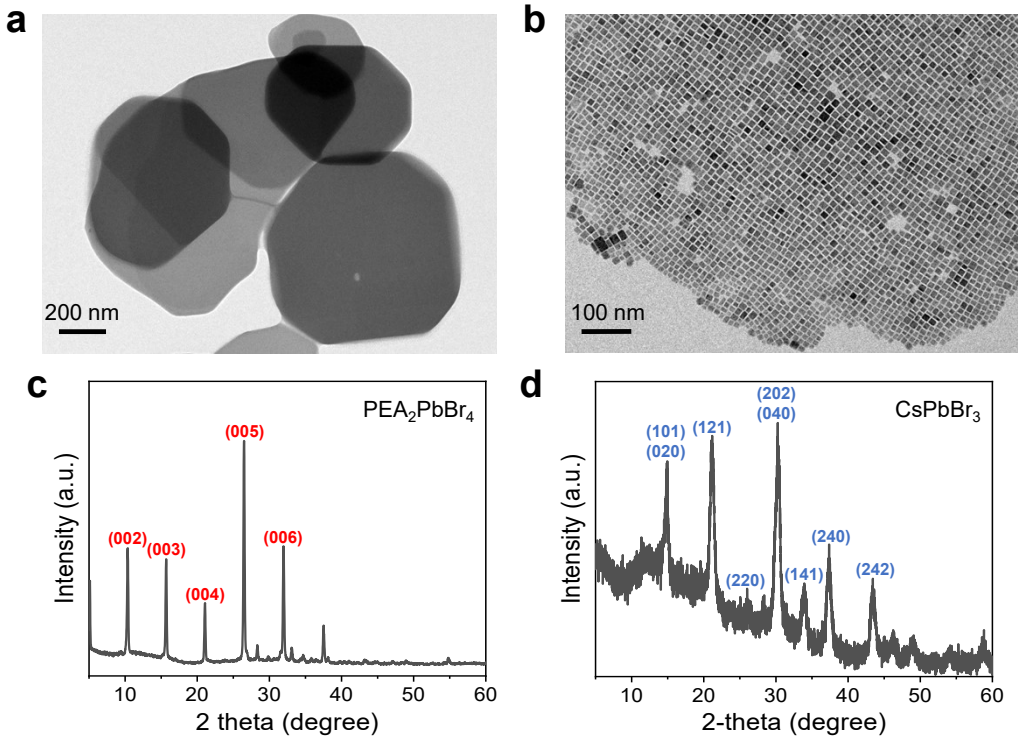

Fig. S7 TEM images of (a) PEA_2PbBr_4 nanoplates and (b) $CsPbBr_3$ nanocubes. XRD patterns of (c) PEA_2PbBr_4 nanoplates and (d) $CsPbBr_3$ nanocubes.

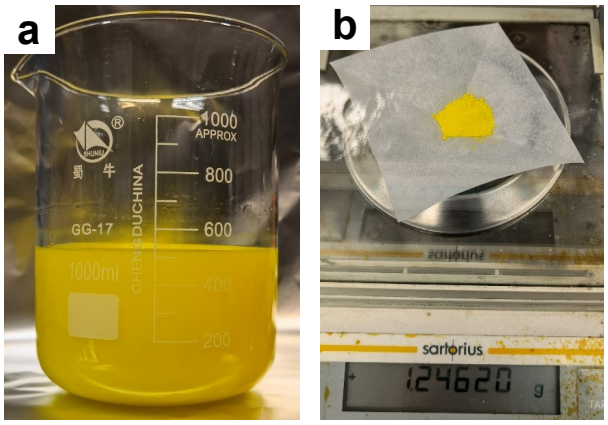

Fig. S8 Photographs of the scalable synthesis of $CsPbBr_3/PEA_2PbBr_4$ heterostructures (a) solution and (b) powder.

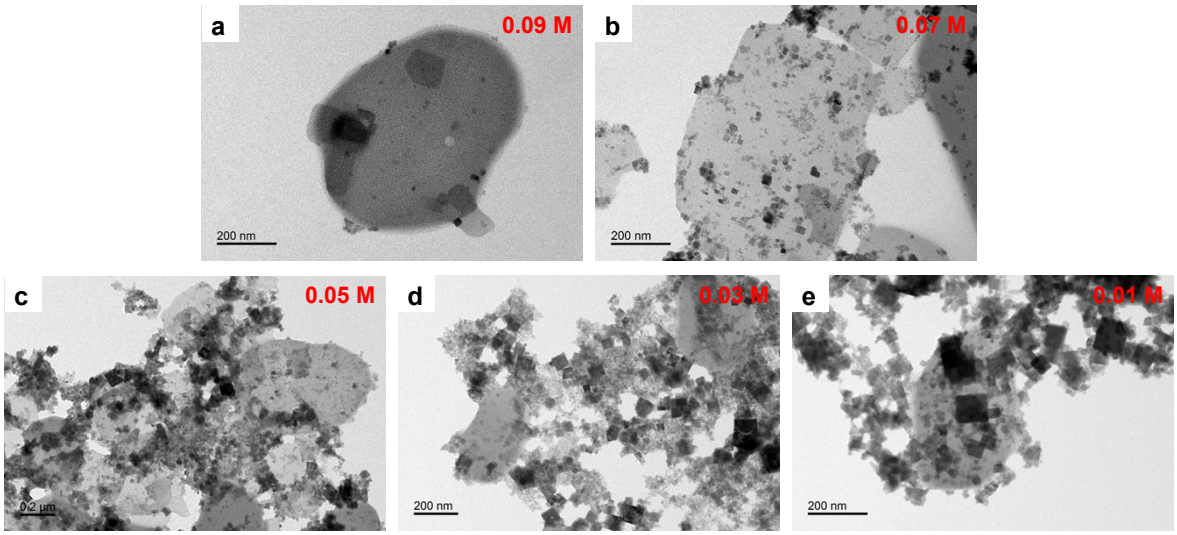

Fig. S9 TEM images of $CsPbBr_3/PEA_2PbBr_4$ heterostructures synthesized with different concentrations of PEABr.

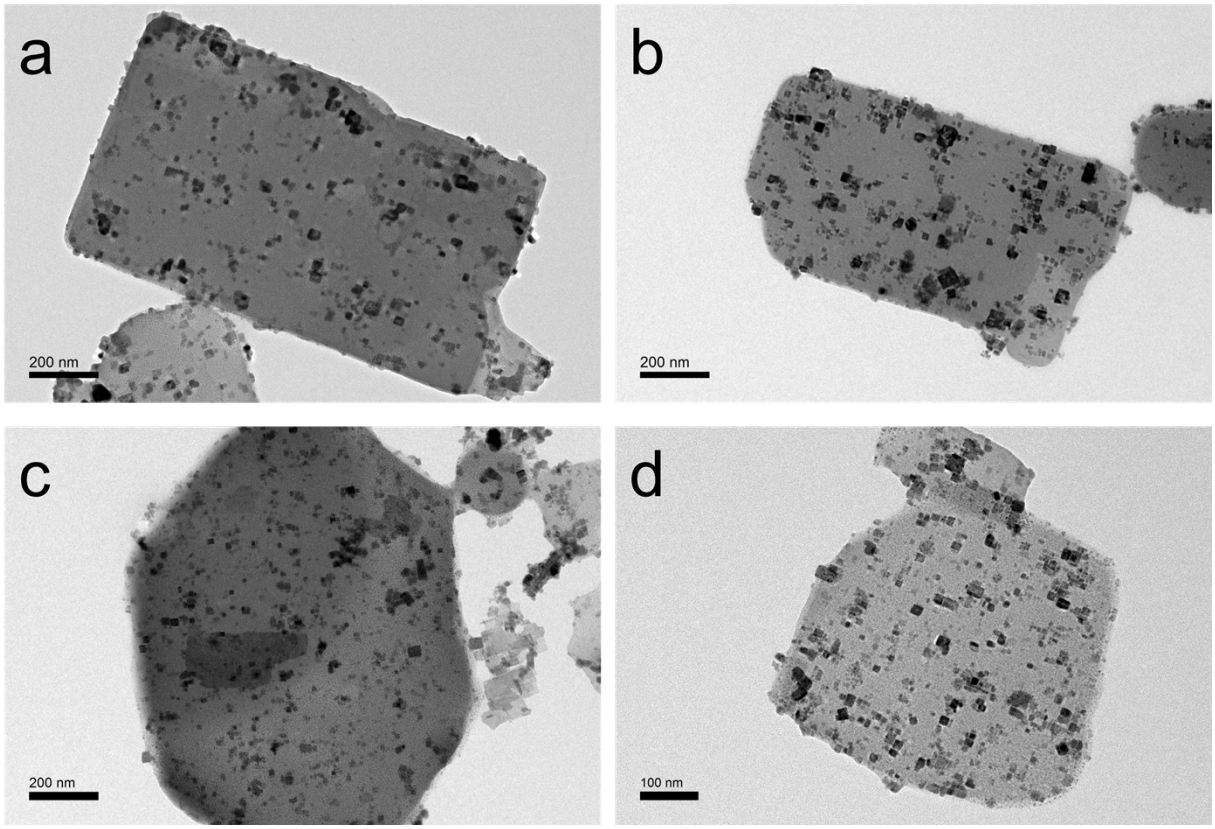

Fig. S10 TEM images of nanoplates and heterostructures based on different anions. (a, b) $CsPb(Cl/Br)_3/PEA_2Pb(Cl/Br)_4$ and (c, d) $CsPb(Br/I)_3/PEA_2Pb(Br/I)_4$.

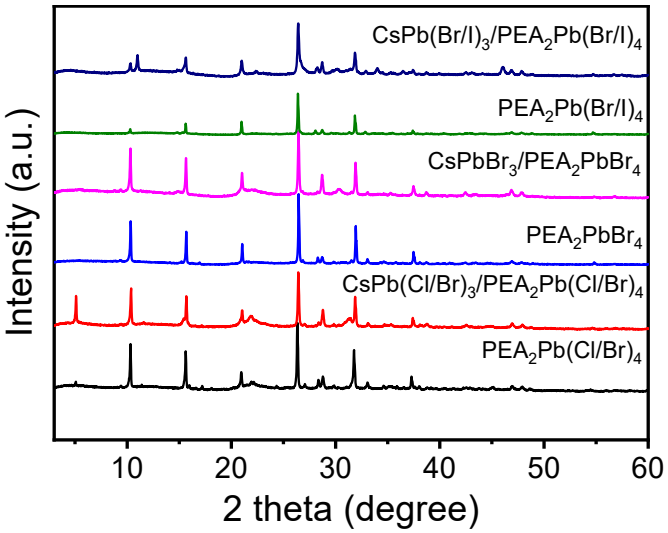

Fig. S11 XRD patterns of nanoplates and heterostructures based on different anions.

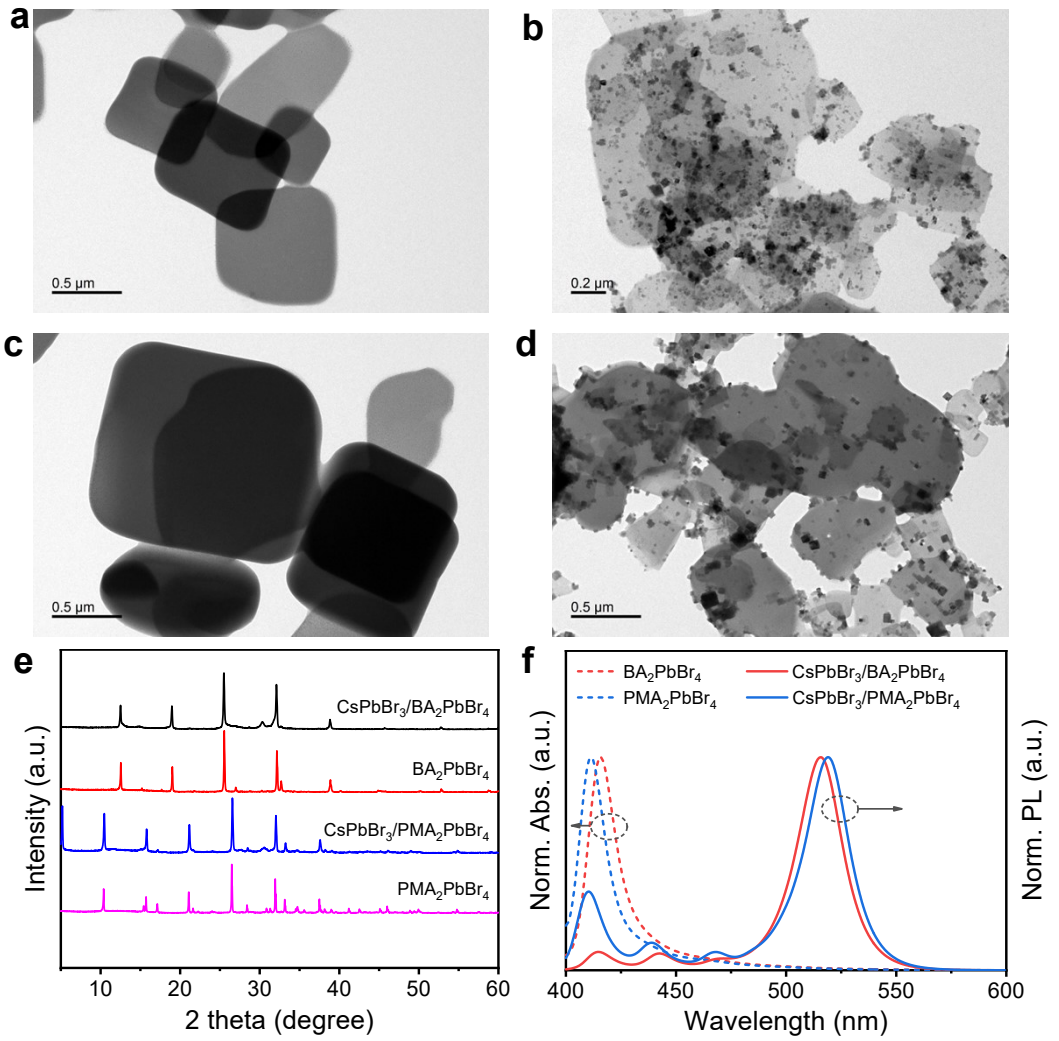

Fig. S12 TEM images of (a) BA_2PbBr_4, (b) $CsPbBr_3/BA_2PbBr_4$, (c) PMA_2PbBr_4 and (d) $CsPbBr_3/PMA_2PbBr_4$ heterostructures. (e) XRD patterns and (f) Absorbance and PL spectra of corresponding nanoplates and heterostructures based on different organic cations.

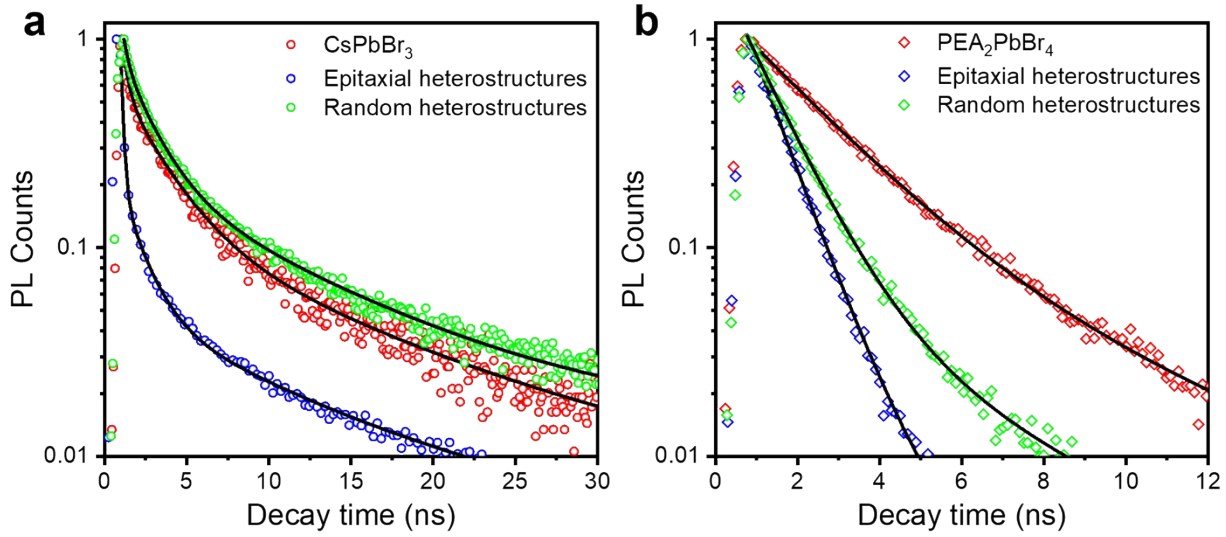

Fig. S13 (a) PL lifetime of $CsPbBr_3$, epitaxial and random $CsPbBr_3/PEA_2PbBr_4$ heterostructures record at emission center of 517 nm under the excitation of 450 nm laser. (b) PL lifetime of PEA_2PbBr_4, epitaxial and random $CsPbBr_3/PEA_2PbBr_4$ heterostructures record at emission center of 415 nm under the excitation of 375 nm laser.

We measured the time-resolved photoluminescence lifetime (TRPL) of both epitaxial and random heterostructures which reveal the effective charge transfer in the epitaxial one. The decay time of bare $CsPbBr_3$ nanocubes, epitaxial and random $CsPbBr_3/PEA_2PbBr_4$ heterostructures at the emission peak of 517 nm under the excitation of 450 nm was measured, respectively (Fig. S13a). The obviously quenching of the emission peak in $CsPbBr_3$ after formation of epitaxial heterostructures was observed due to hole transfer. In sharp contrast, there is no obvious quenching in the case of random heterostructures, which indicates that the hole transfer was largely blocked by the disordered organic ligand layer between $CsPbBr_3$ and PEA_2PbBr_4 (Fig. S5b). It is interesting to note that the lifetime of $CsPbBr_3$ in the random heterostructures was slightly increased. This might be due to the fact that PEA molecules in the PEA_2PbBr_4 solution partly replaced the OLA and OA ligands on $CsPbBr_3$, which led to improved emission stability by the passivation of trap states. The quenching of PEA_2PbBr_4 emission at 415 nm after formation of heterostructures were also investigated (Fig. S13b). Note that under the excitation of 375 nm laser, the quenching of PEA_2PbBr_4 could be attributed to both the electron transfer and energy transfer with $CsPbBr_3$. This is because due to the overlap of the absorption of $CsPbBr_3$ and emission of PEA_2PbBr_4, energy transfer from PEA_2PbBr_4 to $CsPbBr_3$ is possibly existing in the heterostructures. Nevertheless, such quenching in the epitaxial heterostructures was more effective than that in the random heterostructures. Therefore, we can conclude that the charge transfer is more efficient in epitaxial heterostructures.

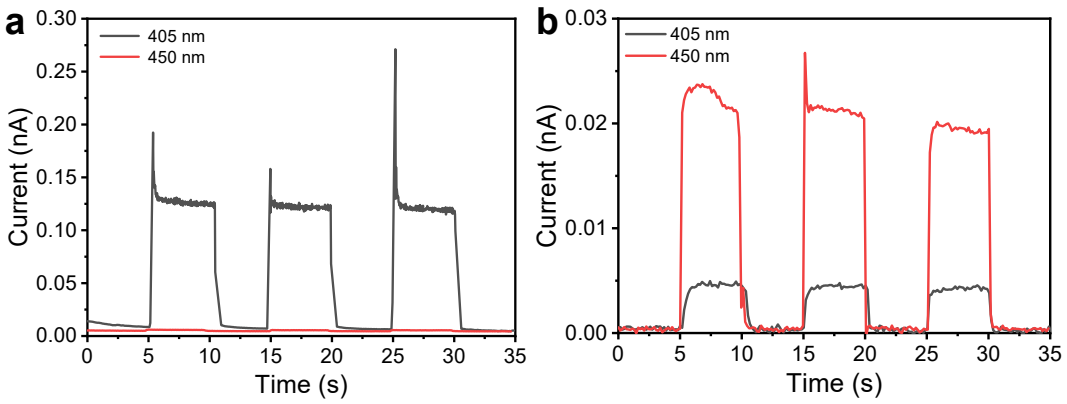

Fig. S14 *I-t* curves of the photodetectors based equal mass loadings as in the heterostructures of (a) PEA_2PbBr_4 nanoplates and (b) $CsPbBr_3$ nanocubes under 405 nm and 450 nm laser illumination with a power density of 4 mW/cm^2.

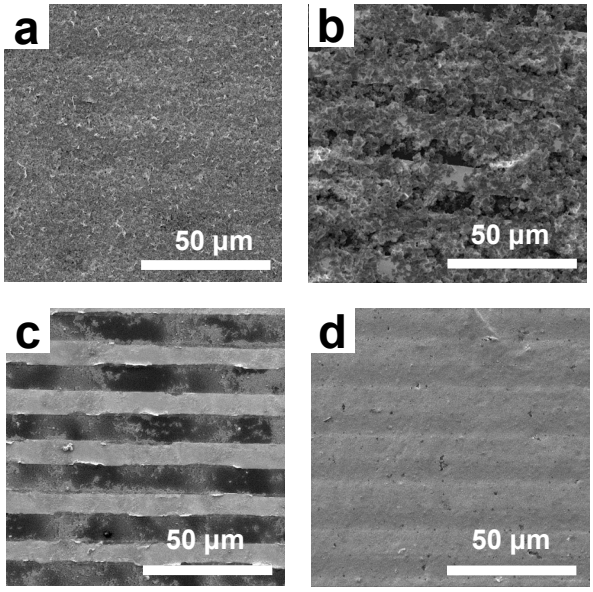

Fig. S15 SEM images of photodetectors based on (a) $CsPbBr_3/PEA_2PbBr_4$ epitaxial heterostructures, (b) PEA_2PbBr_4 nanoplates and (c) $CsPbBr_3$ nanocubes. For PEA_2PbBr_4 and $CsPbBr_3$, their loading amounts are equal to those in the heterostructures. (d) SEM image of photodetector based on $CsPbBr_3$ nanocubes with 30 times of mass loading as compared to that in (c).

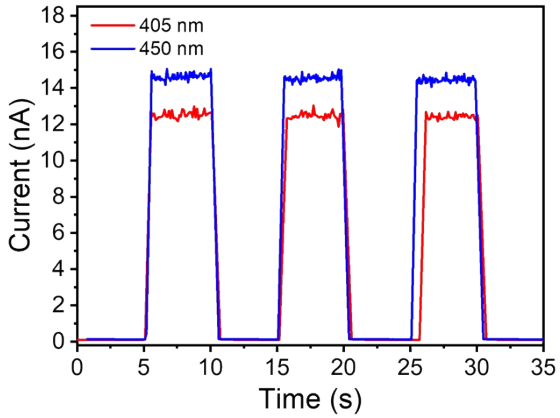

Fig. S16 *I-t* curve of the photodetectors based on 30 times of mass loading of $CsPbBr_3$ nanocubes as compared to that in Fig. S14b under the illumination of 405 and 450 nm laser with an intensity of 4 mW/cm^2.

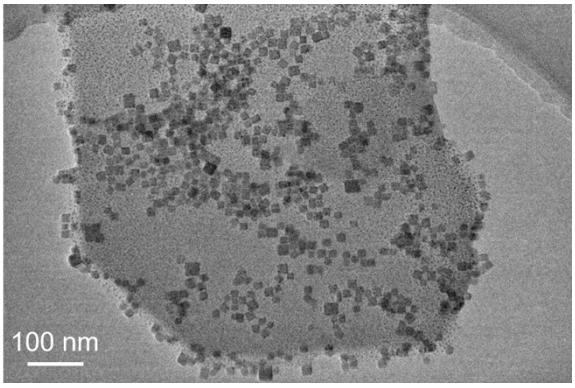

Fig. S17 TEM image of random $CsPbBr_3/PEA_2PbBr_4$ heterostructures.

Table S1. EDX analysis of perovskite nanoplates and heterostructures prepared by anion modulation.

Sample	Pb	Cs	Cl	Br	I
$PEA_2Pb(Cl/Br)_4$	17.4		35.0	47.7	
$CsPb(Cl/Br)_3/PEA_2Pb(Cl/Br)_4$	16.9	4.8	21.9	56.4	
PEA_2PbBr_4	16.4			83.5	
$CsPbBr_3/PEA_2PbBr_4$	16.3	4.3		79.5	
$PEA_2Pb(Br/I)_4$	16.8			75.1	8.9
$CsPb(Br/I)_3/PEA_2Pb(Br/I)_4$	22.8	11.1		52.1	14.1

Table S2. Performance comparison of different photodetectors.

Amount of active layer	Sample	Wavelength	Photoresponsivity (4 mW/cm^2)	On/off ratio
1 time drop-casting with same mass concentration	$CsPbBr_3/PEA_2PbBr_4$ (epitaxial)	405 nm	21.54 μA/W	784.92
		450 nm	10.03 μA/W	250.10
	$CsPbBr_3/PEA_2PbBr_4$ (random)	405 nm	12.26 μA/W	483.91
		450 nm	2.06 μA/W	61.06
1 time drop-casting with same mass concentration as in the heterostructures	$CsPbBr_3$	405 nm	0.17 μA/W	14.51
		450 nm	0.90 μA/W	74.06
	PEA_2PbBr_4	405 nm	3.05 μA/W	14.77
		450 nm	0.15 μA/W	1.28
30 times of repeated drop-casting with mass concentration as in the heterostructures	$CsPbBr_3$	405 nm	240.31 μA/W	140.55
		450 nm	281.89 μA/W	167.01